JOURNAL
OF THE
AMERICAN
CHEMICAL
SOCIETY

Determination of Two Structural Forms of Catalytic Bridging Ligand in Zinc−Phosphotriesterase by Molecular Dynamics Simulation and Quantum Chemical Calculation

Chang-Guo Zhan, Osmar Norberto de Souza, Robert Rittenhouse, and Rick L. Ornstein*

*Contribution from the Pacific Northwest National Laboratory, Battelle-Northwest,
Environmental Technology Division, Mailstop K2-21, Richland, Washington 99352*

Received March 1, 1999

Abstract: Although a three-dimensional X-ray crystal structure of zinc-substituted phosphotriesterase was recently reported, it is uncertain whether a critical bridging ligand in the active site is a water molecule or a hydroxide ion. The identity of this bridging ligand is theoretically determined by performing both molecular dynamics simulations and quantum mechanical calculations. All of the results obtained indicate that this critical ligand in the active site of the reported X-ray crystal structure is a hydroxide anion rather than a water molecule and allow us to propose a dynamic "ping-pong" model in which both kinds of structures might exist.

Introduction

Phosphotriesterase (PTE) from *Pseudomonas diminuta* catalyzes the hydrolysis of organophosphorus pesticides and related nerve agents, i.e., acetylcholinesterase inhibitors, with rate enhancements that approach 10^{12}.[1] There is much current interest in understanding how this remarkable enzyme and related binuclear metal complexes catalyze the hydrolysis so effectively.[2] To elucidate the catalytic mechanism, it is first necessary to determine the structure of the active site. Recently, Vanhooke et al. reported a three-dimensional X-ray crystal structure of zinc-substituted PTE complexed with the substrate analogue, diethyl 4-methylbenzylphosphonate.[3] The X-ray

crystal structure indicates that the two zinc ions in the active site are separated by 3.3 Å. One of the two bridging ligands for the binuclear metal center is a carbamylated Lys (residue 169). It is uncertain whether the other bridging ligand is a water molecule or a hydroxide ion, since hydrogen atoms cannot be determined by X-ray diffraction techniques. It is expected that this second bridging ligand, hydroxide or water, is directly involved in the catalytic hydrolysis process. Here we theoretically determine the identity of this critical bridging ligand by performing both molecular dynamics (MD) simulations on the solvated PTE−inhibitor complex and quantum chemical calculations on simplified models of the active site. On the basis of the theoretical results obtained, a possible dynamic "ping-pong" model is proposed.

Calculation Methods

MD simulations were carried out on subunit 2 of the PTE dimer,[3] using the SANDER module of AMBER 4.1[4] with the force field

* Address correspondence to this author. E-mail: rick.ornstein@pnl.gov. Fax: 509-375-6904. Phone: 509-375-2132.
(1) Dumas, D. P.; Caldwell, S. R.; Wild, J. R.; Raushel, F. M. *J. Biol. Chem.* **1989**, *264*, 19659.
(2) (a) Kuo, J. M.; Chae, M. Y.; Raushel, F. M. *Biochemistry* **1997**, *36*, 1982. (b) Hong, S.-B.; Mullins, L. S.; Shim, H.; Raushel, F. M. *Biochemistry* **1997**, *36*, 9022. (c) Seo, J. S.; Hynes, R. C.; Williams, D.; Chin, J. *J. Am. Chem. Soc.* **1998**, *120*, 9945.
(3) Vanhooke, J. L.; Benning, M. M.; Raushel, F. M.; Holden, H. M. *Biochemistry* **1996**, *35*, 6020.
(4) Pearlman, D. A.; Case, D. A.; Caldwell, J. W.; Ross, W. S.; Cheatham, T. E., III; Ferguson, D. M.; Seibel, G. L.; Singh, U. C.; Weiner, P. K.; Kollman, P. A. *AMBER 4.1*, University of California, San Francisco, 1995.

reported by Cornell et al.[5] A *nonbonded model* was employed to treat zinc ions, with a formal charge of +2. The Lennard-Jones parameters of Zn^{2+} were adapted from Stote and Karplus.[6] We tested these parameters in a simulation of Zn^{2+} in a box of 228 TIP3P water molecules and found that the first (at 2.12 Å) and second (at 4.10 Å) peaks of the radial distribution around the Zn^{2+} are in good agreement with the experimental values[7] 2.05−2.17 and 4.10 Å for the first and second hydration shells, respectively. Simulations of 550 ps were carried out on each of the alternative PTE−inhibitor structures: one with water as the second bridging ligand and the other with the hydroxide anion. Both simulations used a 2.0 fs time step and employed the particle-mesh Ewald (PME) method.[8] Each simulation started from the 2.1 Å resolution X-ray crystal structure.[3] The all-atom models were neutralized by adding two or three chloride counterions for the case of the ligand being hydroxide and water, respectively, and were immersed in rectangular boxes (with initial size of 77.0 Å × 76.0 Å × 79.0 Å) containing a total of 10 785 or 10786 TIP3P water molecules. The simulations were performed with a periodic boundary condition in the NPT ensemble at 300 K with Berendsen temperature coupling[9] and constant pressure (1 atm) with isotropic molecule-based scaling.[9] The SHAKE algorithm,[10] with a tolerance of 10^{-5}, was applied to fix all bonds containing a hydrogen atom, and the nonbond pair list was updated every 10 steps.

Quantum chemical calculations were carried out on three active site models by use of the Gaussian94 program.[11] Their geometries were fully optimized by employing the Hartree−Fock (HF) method with two different basis sets, 3-21G and 6-31G*,[12] and density functional theory using Becke's three-parameter hybrid exchange functional and the Lee−Yang−Parr correlation functional (B3LYP)[13] with 6-31G* basis set. Vibrational frequencies were evaluated at the optimized geometries to verify their true stability and to evaluate the zero-point vibration energies. A second-order Møller−Plesset (MP2) calculation, with 6-31G* basis set, was also performed to fully optimize geometry of the smallest one of the models, to test the reliability of the HF and B3LYP results. Finally, the geometries optimized at the B3LYP/6-31G* level for the two active site models were employed to perform self-consistent reaction field (SCRF) calculations at the HF/6-31G* level, for calculating free energies of solvation in aqueous solution. The calculated free energy in solution was taken as the energy calculated at B3LYP/6-31G* level in gas phase plus the solvent shift calculated at HF/6-31G* level. The SCRF method employed was developed and

Figure 1. Plots of the important internuclear distances versus the simulation time.

Figure 2. Geometries optimized at B3LYP/6-31G* level for the three active site models.

implemented recently in the GAMESS program[14] by one of us (together with Bentley and Chipman),[15a] and may be called the fully polarizable continuum model (FPCM) since both surface and volume polarization effects are fully determined in the SCRF calculation.[15] The FPCM procedure is currently the only general implementation to accurately determine volume polarization (produced by the small amount of the solute charge outside the cavity) for a general irregularly shaped solute cavity in addition to the more commonly treated surface polarization. Since the solute cavity surface is defined as a solute electron charge isodensity contour determined self-consistently during the FPCM iteration process, the FPCM results, converged to the exact solution of Poisson's equation with a given numerical tolerance, depend only on the contour value at a given dielectric constant and a certain quantum chemical calculation level.[15] This single parameter value has been determined as 0.001 au based on an extensive calibration study.[15b]

The quantum chemical calculations and molecular dynamics simulations were all carried out on SGI Origin 200 multiprocessor computers.

Results and Discussion

Let us first discuss the MD results. Depicted in Figure 1 are plots of the simulated internuclear distances between the two zinc ions (Zn1 and Zn2), and between the zinc ions and the oxygen (O1) in the examined bridging ligand (hydroxide or water) versus the simulation time. The plot for the hydroxide simulation indicates that the time-average values for both the Zn1−O1 and Zn2−O1 distances are in excellent agreement with the experimental value of 2.0 Å (for both). The average value

(5) (a) Cornell, W. D.; Cieplak, P.; Bayly, C. I.; Gould, I. R.; Merz, K. M., Jr.; Ferguson, D. M.; Spellmeyer, D. C.; Fox, T.; Caldwell, J. W.; Kollman, P. A. *J. Am. Chem. Soc.* **1995**, *117*, 5179. (b) The RESP charges in the carbamylated Lys 169 and diethyl 4-methylbenzylphosphonate were determined by ourselves following the standard RESP procedure described in ref 5a. The bond and rotational parameters of a carboxylic group were used for the carbamylate end of Lys 169, and the bond and rotational parameters for the methoxy groups in the inhibitor were modeled on the basis of the parameters for the phosphate group of nucleic acid.

(6) Stote, R. H.; Karplus, M. *Proteins* **1995**, *23*, 12.

(7) (a) Ohtaki, H.; Yamaguchi, T.; Maeda, M. *Bull. Chem. Soc. Jpn.* **1976**, *49*, 701. (b) Johansson, G. *Adv. Inorg. Chem.* **1992**, *39*, 159.

(8) Essmann, U.; Perera, L.; Berkowitz, M. L.; Darden, T. A.; Lee, H., Pedersen, L. G. *J. Chem. Phys.* **1995**, *103*, 10089.

(9) Berendsen, H. C.; Postma, J. P. M.; van Gunsteren, W. F.; DiNola, A.; Haak, J. R. *J. Comput. Phys.* **1984**, *81*, 3684.

(10) Ryckaert, J. P.; Ciccotti, G.; Berendsen, H. C. *J. Comput. Phys.* **1977**, *23*, 327.

(11) Frisch, M. J.; Trucks, G. W.; Schlegel, H. B.; Gill, P. M. W.; B. G. Johnson, B. G.; Robb, M. A.; Cheeseman, J. R.; Keith, T.; Petersson, G. A.; Montgomery, J. A.; Raghavachari, K.; Al-Laham, M. A.; Zakrzewski, V. G.; Ortiz, J. V.; Foresman, J. B.; Cioslowski, J.; Stefanov, B. B.; Nanayakkara, A.; Challacombe, M.; Peng, C. Y.; Ayala, P. Y.; Chen, W.; Wong, M. W.; Andres, J. L.; Replogle, E. S.; Gomperts, R.; Martin, R. L.; Fox, D. J.; Binkley, J. S.; Defrees, D. J.; Baker, J.; Stewart, J. P.; Head-Gordon, M.; Gonzalez, C.; Pople, J. A. *Gaussian 94*, Revision D.1, Gaussian, Inc., Pittsburgh, PA, 1995.

(12) (a) Hariharan, P. C.; Pople, J. A. *Theor. Chim. Acta* **1973**, *28*, 213. (b) Rassolov, V. A.; Pople, J. A.; Ratner, M. A.; Windus, T. L. *J. Chem. Phys.* **1998**, *109*, 1223.

(13) (a) Becke, A. D., *J. Chem. Phys.* **1993**, *98*, 5648. (b) Lee, C.; Yang, W.; Parr, R. G. *Phys. Rev. B* **1988**, *37*, 785.
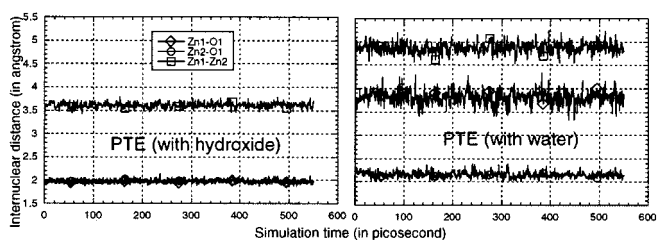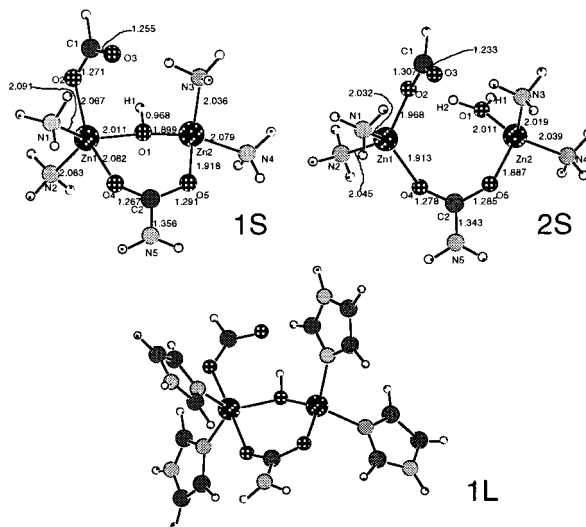
(14) Schmidt, M. W.; Baldridge, K. K.; Boatz, J. A.; Elbert, S. T.; Gordon, M. S.; Jensen, J. H.; Koseki, S.; Matsunaga, N.; Nguyen, K. A.; Su, S. J.; Windus, T. L.; Dupuis, M.; Montgomery, J. A. *J. Comput. Chem.* **1993**, *14*, 1347.

(15) (a) Zhan, C.-G.; Bentley, J.; Chipman, D. M. *J. Chem. Phys.* **1998**, *108*, 177. (b) Zhan, C.-G.; Chipman, D. M. *J. Chem. Phys.* **1998**, *109*, 10543. (c) Zhan, C.-G.; Chipman, D. M. *J. Chem. Phys.* **1999**, *110*, 1611. (d) Dielectric constant used in this study for aqueous solution is 78.5.

Table 1. Important Internuclear Distances (Å) Optimized at Various Calculation Levels

distance	model molecule 1L			model molecule 1S				model molecule 2S			expt.[3] (X-ray)
	HF3-21G	HF6-31G*	B3LYP6-31G*	HF3-21G	HF6-31G*	B3LYP6-31G*	MP26-31G*	HF3-21G	HF6-31G*	B3LYP6-31G*	
Zn1−O1	1.915	1.963	1.940	1.959	2.045	2.011	2.002	3.801	3.888	3.750	2.0
Zn1−O2	2.086	2.085	2.104	2.064	2.065	2.082	2.057	1.922	1.967	1.968	2.3
Zn1−O4	2.101	2.222	2.220	1.997	2.077	2.082	2.081	1.862	1.932	1.913	2.2
Zn1−N1	2.024	2.121	2.057	2.068	2.182	2.091	2.078	2.022	2.083	2.032	1.9
Zn1−N2	1.997	2.085	2.026	2.042	2.150	2.083	2.072	2.019	2.095	2.045	2.0
Zn2−O1	1.858	1.893	1.881	1.868	1.901	1.899	1.901	1.937	2.055	2.011	2.0
Zn2−O5	1.909	1.954	1.945	1.890	1.932	1.918	1.917	1.859	1.895	1.887	1.8
Zn2−O3	1.985	2.072	2.028	2.007	2.085	2.036	2.020	2.013	2.058	2.019	2.0
ZnC−N4	1.987	2.073	2.029	2.037	2.127	2.079	2.064	2.020	2.089	2.039	2.1
O4−C2	1.261	1.238	1.258	1.264	1.245	1.267	1.270	1.275	1.254	1.278	1.2
O5−C2	1.284	1.265	1.289	1.287	1.265	1.291	1.295	1.277	1.262	1.285	1.3
C2−N5	1.347	1.354	1.378	1.335	1.341	1.356	1.356	1.325	1.328	1.343	1.5
O2−C1	1.276	1.257	1.276	1.268	1.247	1.271	1.277	1.318	1.280	1.307	1.3
C1−O3	1.245	1.222	1.249	1.256	1.233	1.256	1.263	1.226	1.212	1.233	1.2
Zn1−Zn2	3.337	3.411	3.353	3.257	3.271	3.261	3.248	4.285	4.304	4.195	3.3

for the Zn1−Zn2 distance in the simulation, about 3.6 Å, is also close to the experimental value of 3.3 Å.[3] These results indicate that the hydroxide remains coordinated to both zinc ions throughout the simulation. The simulation on the structure containing the bridging water molecule produced very different results. The time-averaged Zn1−O1, Zn2−O1, and Zn1−Zn2 distances quickly converged to values of about 3.8, 2.2, and 4.8 Å, respectively. These values are qualitatively different from the experimental data. Obviously, the water molecule coordinated only to one zinc according to the MD results. Therefore, the MD simulations indicate that the second bridging ligand in the X-ray structure is a hydroxide anion instead of a water molecule.

Are the MD simulations, with an empirical force field, reliable for studying the problem at hand? The qualitative results of the MD simulations can be tested through comparison with quantum chemical calculations. As depicted in Figure 2, we examined the three active site models denoted by 1S, 1L, and 2S. 1S is a small active-site model in which the second bridging ligand is considered as a hydroxide anion and the His 55, His 57, His 201, and His 230 residues are all simplified as NH_3 molecules. Table 1 reveals that the internuclear distances involving zinc determined at the different levels of theory are close to each other and are all qualitatively consistent with the corresponding experimental values and the MD results. The small difference between the HF/3-21G and HF/6-31G* results indicate that the 6-31G* basis set employed is sufficiently large. The minor differences among the HF/6-31G*, B3LYP/6-31G* and MP2/6-31G* results indicate that electron correlation effects on the geometry optimization are not important and that density functional theory with the B3LYP functional gives results very close to the results of the much more expensive MP2 calculation including electron correlation. 1L is a larger model where each NH_3 is replaced by imidazole with a hydroxide employed to theoretically examine the suitability of model 1S. All three models have the carbamylated lysine and aspartic acid functional group replaced by CO_2NH_2 and CHO_2, respectively. The calculated results do not change significantly from 1S to 1L, thus indicating that model 1S is sufficient for our purpose. The optimized Zn1−O1, Zn2−O1, and Zn1−Zn2 distances in both 1S and 1L are all in excellent agreement with the experimental values. 2S is a small model, considering the second bridging ligand as a water molecule. The initial guess used for the 2S geometry optimization was constructed from the optimized structure of the 1S model, in which the hydroxide anion is changed into a water molecule by adding an additional proton.
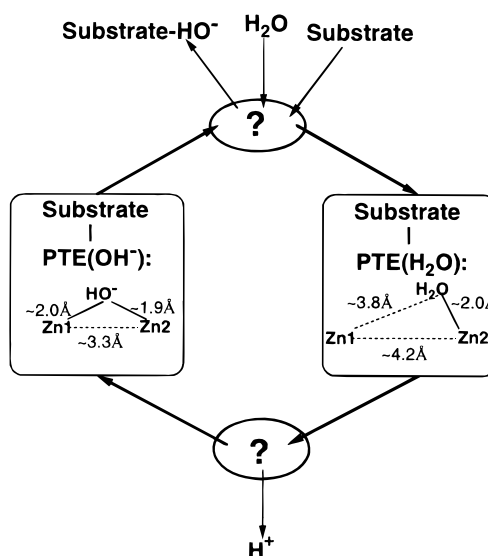
Figure 3. Proposed dynamic "ping-pong" model in which both kinds of structures might exist.

It turns out that the optimized geometry of 2S is qualitatively different from that of 1S. The hydroxide in 1S coordinates to the two zinc ions simultaneously, while the water in 2S coordinates only to one zinc. These results are qualitatively coincident with the MD results described above and strongly support the conclusion that the second bridging ligand in the active site of the reported X-ray crystal structure of PTE is a hydroxide anion rather than a water molecule.

Comparison of the optimized geometries for the 1S and 2S models, along with the corresponding MD results, allows one to imagine a dynamic ping-pong model, as depicted in Figure 3, in which both kinds of structures might exist. The active site of PTE may first accept a water molecule which coordinates only to one zinc and, following proton transfer from the water (the zinc-bound water) to a nearby residue, the zinc-bound water molecule becomes a zinc-bound hydroxide anion, which coordinates to the nearby second zinc resulting in a contraction of the Zn1−Zn2 distance by about 1 Å. Then the hydroxide anion may attack the substrate to initiate hydrolysis. After hydrolysis and product release, another water molecule could enter the active site to repeat the cycle. When the substrate is replaced by the inhibitor, as in the PTE X-ray structure, hydrolysis is unable to occur, since no acceptable leaving group is present; the bond orientation of the inhibitor is also not suitable for a functional leaving group. The enzyme thus cannot function, and

the active site is locked into a stable structure that can be determined experimentally; in this case, the structure with a bridging hydroxide anion.

It is interesting to theoretically estimate the pK_a value of the catalytic bridging ligand. For this purpose, we consider the free energy change ΔG_a for the model reaction

$$2S \text{ (solvated)} \rightarrow 1S \text{ (solvated)} + H^+ \text{ (solvated)} \quad (1)$$

By employing the free energies calculated for 2S and 1S and the experimental data for a proton as used by Lim, Bashford, and Karplus,[16] we get $pK_a = \Delta G_a/(2.303RT) = 5.9$ when $T = 298$ K, which is very close to the experimental pK_a value, 5.8, determined for the zinc-substituted PTE by a kinetic method.[17] This calculated pK_a value indicates that when the pH value is about 5.9, the concentrations of the two kinds of PTE active-site structures (with hydroxide and with water) should be equal to each other. At lower pH the PTE active-site structure with water should be dominant, and at higher pH the PTE active-site structure with the catalytic bridging hydroxide should be dominant. Thus, the concentration of the PTE active-site structure with the catalytic bridging hydroxide is a function of the pH, which qualitatively explains the observed pH dependence of the PTE activity.[17,18]

Another interesting issue of the PTE active-site structure is the metal dependence. It has been reported that this enzyme accepts Zn^{2+}, Cd^{2+}, Mn^{2+}, Co^{2+} and Ni^{2+}.[19] Could similar active-site structures with the catalytic bridging hydroxide and water exist when the Zn^{2+} ions are replaced by other metal ions? Replacement of Zn^{2+} ions with other divalent metal ions is expected to lead to quantitative changes in the coordination numbers and in the pK_a of the catalytic bridging ligand because of the changes in ionic radius or/and in number of valence electrons of the metal ion. Active-site structures of PTE with other metal ions could also be theoretically identified.

Conclusion

The present results obtained from molecular dynamics simulations and quantum chemical calculations strongly support the conclusion that the second bridging ligand in the active site of the reported X-ray crystal structure of PTE is a hydroxide anion rather than a water molecule. On the basis of these theoretical results, a dynamic ping-pong model, in which both kinds of structures might exist, is proposed.

(16) Lim, C.; Bashford, D.; Karplus, M. *J. Phys. Chem.* **1991**, *95*, 5610.
(17) Omburo, G. A.; Kuo, J. M.; Mullins, L. S.; Raushel, F. M. *J. Biol. Chem.* **1992**, *267*, 13278.
(18) Donarski, W. J.; Dumas, D. P.; Heitmeyer, D. P.; Lewis, V. E.; Raushel, F. M. *Biochemistry* **1989**, *28*, 4650.

(19) Hong, S.-B.; Raushel, F. M. *Biochemistry* **1996**, *35*, 10904.